



**HAL**  
open science

## **N<sup>-3</sup> azide anion confined inside finite-size carbon nanotubes**

Stefano Battaglia, Stefano Evangelisti, Noelia Faginas Lago, Thierry Leininger

► **To cite this version:**

Stefano Battaglia, Stefano Evangelisti, Noelia Faginas Lago, Thierry Leininger. N<sup>-3</sup> azide anion confined inside finite-size carbon nanotubes. *Journal of Molecular Modeling*, 2017, 23 (10), pp.294. 10.1007/s00894-017-3468-8 . hal-01657201

**HAL Id: hal-01657201**

**<https://hal.science/hal-01657201>**

Submitted on 5 Oct 2018

**HAL** is a multi-disciplinary open access archive for the deposit and dissemination of scientific research documents, whether they are published or not. The documents may come from teaching and research institutions in France or abroad, or from public or private research centers.

L'archive ouverte pluridisciplinaire **HAL**, est destinée au dépôt et à la diffusion de documents scientifiques de niveau recherche, publiés ou non, émanant des établissements d'enseignement et de recherche français ou étrangers, des laboratoires publics ou privés.

# ACCEPTED MANUSCRIPT

The final publication is available at [link.springer.com](https://link.springer.com) at the following link:  
<https://link.springer.com/article/10.1007/s00894-017-3468-8>

DOI: <https://doi.org/10.1007/s00894-017-3468-8>

# $N_3^-$ Azide Anion Confined Inside Finite-Size Carbon Nanotubes

**Stefano Battaglia · Stefano Evangelisti ·**

**Noelia Faginas-Lago · Thierry Leininger**

Received: date / Accepted: date

---

Stefano Battaglia

Laboratoire de Chimie et Physique Quantiques, IRSAMC, Université Paul Sabatier, 118 Route  
de Narbonne, F-31062 Toulouse Cedex - France

Dipartimento di Chimica, Biologia e Biotecnologie, Università degli Studi di Perugia, Vie Elce  
di Sotto 8, I-06123 Perugia, Italy

Stefano Evangelisti

Laboratoire de Chimie et Physique Quantiques, IRSAMC, Université Paul Sabatier, 118 Route  
de Narbonne, F-31062 Toulouse Cedex - France

Noelia Faginas-Lago

Dipartimento di Chimica, Biologia e Biotecnologie, Università degli Studi di Perugia, Vie Elce  
di Sotto 8, I-06123 Perugia, Italy

Thierry Leininger

Laboratoire de Chimie et Physique Quantiques, IRSAMC, Université Paul Sabatier, 118 Route  
de Narbonne, F-31062 Toulouse Cedex - France

Tel.: +33 (0)5 61 55 61 52

E-mail: [Thierry.Leininger@irsamc.ups-tlse.fr](mailto:Thierry.Leininger@irsamc.ups-tlse.fr)

**Abstract** In this work, the confinement of an  $\text{N}_3^-$  azide anion inside finite-size single-wall zigzag and armchair carbon nanotubes of different diameters has been studied by wave function and density functional theory. Unrelaxed and relaxed interaction energies have been computed, resulting in a favorable interaction between the guest and host system. In particular, the largest interaction has been observed for the confinement in an armchair (5,5) carbon nanotube, for which a natural population analysis as well as an investigation based on the molecular electrostatic potential has been carried out. The nature of the interaction between the two fragments appears to be mainly electrostatic, favored by the enhanced polarizability of the nanotube wall treated as a finite system and passivated by hydrogen atoms. The results obtained are promising for possible applications of this complex as a starting point for the stabilization of larger polynitrogen compounds, suitable as a high-energy density material.

**Keywords** Carbon Nanotubes · HEDM · Polynitrogen Compound · Azide Anion · Molecular Confinement

## 1 Introduction

In the search for alternative energy sources and environmentally friendly fuels, polynitrogen compounds (PNCs) exhibit a high potential of success due to the amount of energy released by their decomposition into inert  $\text{N}_2$  molecules and they have thus been proposed as possible high-energy density material (HEDM)[1,2]. Among them, probably the most famous one is the  $\text{N}_3^-$  azide anion known since the end of the nineteenth century[3], which has regained much attention after the successful synthesis of the  $\text{N}_5^+$  cation[4], envisioning the pure nitrogen salt  $\text{N}_3^- \text{N}_5^+$ [5,

6,7,8]. Considering PNCs as HEDM, the illustrative example of the energy stored in the ionic cluster N<sub>3</sub><sup>-</sup>N<sub>5</sub><sup>+</sup> is emblematic, where upon dissociation into four N<sub>2</sub> molecules, the release of energy is around 70 kcal/mol per mole of N<sub>2</sub>[7].

Despite the efforts, the main difficulty still remains the intrinsic instability of PNCs, which at ambient conditions mostly dissociate into N<sub>2</sub> directly or overcoming a low energy barrier. A recently proposed approach predicted the stabilization of an N<sub>8</sub> chain through molecular confinement inside carbon nanotubes (CNTs)[9, 10], for which it has been shown that the polymeric nitrogen form is stable at ambient conditions when it resides inside the nanotube cavity. Additional studies considering several N<sub>8</sub> chains confined in a carbon nanotube bundle and the confinement inside boron nitride nanotubes have obtained similar results[11,12]. Experimentally, it has been possible to stabilize an N<sub>8</sub><sup>-</sup> anionic species on multi-wall CNTs at ambient conditions, although not with the goal of energy storage[13]. A comprehensive theoretical study by density functional theory (DFT) on nitrogen clusters with different number of atoms encapsulated in a C<sub>60</sub> fullerene has been carried out too, predicting stable structures up to 13 atoms before starting to be incorporated in the confining cage[14]. Confinement inside carbon nanostructures has not been explored only for PNCs, but for other types of molecular clusters too; most notably for Ga<sub>n</sub> and Al<sub>n</sub> clusters, for which increased stabilization and new isomers have been found for the encapsulated species[15,16].

The success of this approach has led us to this contribution, in which we propose to confine the simplest nitrogen compound beyond N<sub>2</sub>, the N<sub>3</sub><sup>-</sup> azide anion, inside single-wall finite-size carbon nanotubes of different diameters. From a theoretical perspective, using *ab-initio* molecular orbital theory, we investigate the effects of the encapsulation by computing (un-)relaxed interaction energies using both den-

sity functional theory (DFT) and wave function theory (WFT) and we study the effects on both the guest nitrogen species and the host carbon structure by means of atomic charges and molecular electrostatic potentials (MEPs). The article is organized as follows. In the Computational Details Section we describe the methodology used to perform the calculations, in the Results Section we show the results obtained in this study and at last, in the Conclusions Section we finalize this work by summarizing and highlighting the most important findings.

## 2 Computational Details

In this work, single-wall carbon nanotubes have been treated as finite-size systems, passivated on both edges by the addition of one hydrogen atom for each terminal carbon atom. Two classes of CNTs have been considered, namely  $(n,0)$  zigzag and  $(m,m)$  armchair CNTs, with values of  $n$  equal to 8, 10 and 12, and values of  $m$  equal to 4, 5 and 6. The length of the tubes was of  $\approx 13.57 \text{ \AA}$  for  $(n,0)$  CNTs and  $\approx 15.43 \text{ \AA}$  for  $(m,m)$  CNTs. The geometries of both types have been relaxed using restricted density functional theory using the three-parameter Becke exchange energy functional[17,18] and the Lee-Yang-Parr correlation energy functional[19] (RB3LYP), optimizing the lowest energy state at this level of theory (triplet state for zigzag CNTs and singlet state for armchair CNTs). Similarly, the trinitrogen anion has also been optimized using RB3LYP. The basis set used for all calculations is the double- $\zeta$  6-31G basis set[20], with the addition of polarization and diffuse functions (6-31+G\*) on the nitrogen atoms. Note that polarization functions on the carbon atoms do not affect qualitatively the results (with errors within  $\approx 2.5$  kcal/mol) and therefore they were not included in the systematic calculations

carried out in this work.

The interaction energy has been calculated in two ways, listed as follows

$$E_{int}^{unrel} = E_{tot} - E_{cnt} - E_{N_3^-}, \quad (1)$$

$$E_{int}^{rel} = \tilde{E}_{tot} - \tilde{E}_{cnt} - \tilde{E}_{N_3^-}, \quad (2)$$

where the presence of a tilde means that the single point calculation has been performed on the geometry obtained by relaxing the entire system, and its absence implies that the geometries used were optimized for the single fragments alone. The basis set superposition error has been taken into account by the counterpoise correction procedure by Boys and Bernardi[21].

The total and fragment energies have been computed with second-order  $n$ -electron valence perturbation theory (NEVPT2) on top of a complete active space self-consistent field (CASSCF) calculation in the case of zigzag CNTs, and with second-order Møller-Plesset perturbation theory (MP2) in the case of armchair nanotubes. The reason behind the application of different methodologies is the open-shell character of the ground state of  $(n,0)$  nanotubes, which requires a multireference approach in order to properly account for the *static* correlation effects. To compute relaxed interaction energies, the systems involving armchair nanotubes have been relaxed using DFT with the dispersion-corrected APFD exchange-correlation energy functional[22], which best reproduced the MP2 unrelaxed interaction energies. The results obtained on the fully relaxed structures have been computed using both DFT and MP2 perturbation theory. All calculations involving zigzag nanotubes have been performed using the 2015.1 version of the MOLPRO program package[23,24] and applying, while all those involving armchair nanotubes with the Gaussian09 suite of programs[25] and the built-in NBO

program[26]. The calculations using Gaussian09 have been performed setting the “Integral” option to “Ultrafine”. The figures appearing in this article have been produced using either the avogadro program version 1.2.0[27,28], or GaussView version 5[29].

### 3 Results

At first, unrelaxed interaction energies have been computed by placing the  $N_3^-$  ion exactly in the center of the nanotube (i.e. the center of the  $xy$ -plane cutting the nanotube), aligned to its principal axis and with the central nitrogen atom in the nanotube midpoint (see Fig. 1). The resulting energies for CNTs of different dimensions and classes are depicted in Fig. 2. For all diameters considered, the interaction is favorable (i.e negative) and thus the nanotube has a stabilizing effect on the confined  $N_3^-$  ion. Although the computational methods employed for the two classes of nanotubes are not the same, the interaction energy “smoothly” varies with respect to the diameter suggesting that the nanotube class does not affect significantly the interaction between the guest and the host system. This result is of particular interest since it implies that the structural pattern of the nanotube wall does not play a role for this kind of “weak” interactions.

The strongest stabilization is found for CNTs with a diameter comprised between 6.26 Å and 6.78 Å, with interaction energies of about  $\approx -31$  kcal/mol. A small (6, 0) CNT was tested too (diameter of 4.70 Å), but the positive interaction energy of more than 100 kcal/mol clearly indicated that the cavity is too small to host the  $N_3^-$  fragment. Nanotubes larger than the (12, 0) one were not considered since the behavior of the interaction energy appears clear. In theory, by keeping the

N<sub>3</sub><sup>-</sup> molecule fixed at the center of the nanotube while increasing its diameter, the interaction energy should decrease and approach zero when the CNT wall is so far away that the nitrogen ion does not feel their influence anymore.

The (5, 5) CNT has the largest stabilizing effect and thus for this case the full system has been relaxed using restricted DFT with APFD functional. The geometry optimization has been started from 6 different orientations of the N<sub>3</sub><sup>-</sup> moiety inside the nanotube as depicted in Fig. 3, in order to ensure that the system does not fall into a too high local minimum. The geometry of Fig. 3a is the same used in the unrelaxed calculation, and upon optimization the position of N<sub>3</sub><sup>-</sup> remains virtually unchanged. The relaxation of starting geometries depicted from Fig. 3b to Fig. 3d yields final structures similar to that of Fig. 3a, where the anion is in the center of the nanotube, slightly displaced from its midpoint along the principal axis. In geometries shown in Figs. 3e and 3f, the N<sub>3</sub><sup>-</sup> moiety was initially displaced towards one end of the nanotube besides being rotated and moved closer to the wall as in the previous cases. Interestingly, also in this latter case the relaxed structures are very similar to the previous ones; during optimization the N<sub>3</sub><sup>-</sup> ion moves towards the midpoint of the nanotube instead of remaining near the edge (see Fig. 4).

Each relaxed geometry is different. In all cases the N<sub>3</sub><sup>-</sup> fragment lies almost perfectly in the center of the CNT, with deviations of at most 0.03 Å from the principal axis. In contrast, its relative position along the axis varies much more among the obtained geometries and in the extremest case the central nitrogen atom is displaced by 0.43 Å from the midpoint of the CNT. Despite these differences in the relaxed structures, energetically they lie all very close to each other, with a maximum difference of merely 0.05 kcal/mol.

It is possible that the geometry relaxation induces considerable changes in the

interaction energy of different nanotubes than the (5,5) CNT, therefore systems involving a (4,4) CNT and a (6,6) CNT have been relaxed too, starting from a single geometry similar to the one depicted in Fig. 3f. For the small (4,4) CNT, the final position of the anion is in the center of the nanotube parallel to the principal axis, displaced by 0.7 Å towards one end of it. In the case of the (6,6) CNT, because of the considerably larger cavity, the  $\text{N}_3^-$  fragment attracted to the nanotube wall moves out of the principal axis and stabilize itself at a distance of  $\approx 3.10$  Å, remaining parallel too it (see Fig. 5).

For these two geometries and the lowest-energy conformation involving the (5,5) CNT, relaxed MP2 interaction energies have been computed and compared to the APFD results, as it is shown in Fig. 6. The energies obtained with the different methods agree very well, with the largest difference of  $\approx 2.60$  kcal/mol obtained for the (4,4) CNT. The comparison with the unrelaxed interaction energies also shows a good agreement; the best interaction (at MP2 level of theory) is maintained by the (5,5) CNT, slightly decreasing from  $-31.12$  kcal/mol to  $-32.31$  kcal/mol, whereas for the other two nanotubes it decreases by  $\approx 2.5$  kcal/mol. Thus, the relaxation process does not change qualitatively the results obtained for the unrelaxed structures. Most likely, one can expect the relaxation to affect more nanotubes with a large diameter, since by fixing the  $\text{N}_3^-$  ion in the center of the nanotube would quickly decrease the interaction energy to zero as the diameter increases, while allowing for structural relaxation would give the  $\text{N}_3^-$  fragment the freedom to be absorbed on the inner side of the nanotube wall, attaining the interaction energy of an  $\text{N}_3^-$  ion absorbed on a graphene sheet in the limit of an infinitely large CNT. It is interesting to note that the distance from the  $\text{N}_3^-$  ion to the (5,5) CNT wall ranges between 3.45 Å and 3.50 Å, which is slightly more

than the optimal absorption distance measured for the (6,6) CNT, i.e.  $\approx 3.10$  Å. The nanotube has virtually no influence on the geometry of the N<sub>3</sub><sup>-</sup> ion; it remains perfectly linear and its bond length decreases by only 0.001 Å for all starting geometries, whereas the deformation energy observed never exceeds 0.01 kcal/mol. In a similar way, the CNT distortion due to the presence of N<sub>3</sub><sup>-</sup> has been quantified to be to at most 0.4 kcal/mol.

The charge distribution on the N<sub>3</sub><sup>-</sup> ion is also minimally affected by the presence of the nanotube. Partial atomic charges on the nitrogen monomer have been computed through a natural population analysis[30] for the simple system in gas phase and for the full complex. The analysis for the monomer shows an excess of 0.14 positive charge on the central nitrogen atom, and an accumulation of negative charge equal to  $-0.57$  on the two external nitrogen atoms. This distribution changes weakly after relaxation of the complex system, with the partial charge on the central atom decreasing to 0.12 and increasing to  $-0.55$  on the two external nitrogen atoms (see Fig. 7). Of particular interest are the electrostatic effects induced by the presence of the negatively charged species inside the nanotube cavity. In this respect, the partial atomic charges on the nanotube change sign in the region of the N<sub>3</sub><sup>-</sup> moiety. The molecular electrostatic potential (MEP) of the nanotube electron density has been plotted for the isolated system and compared to the MEP obtained with the electron density influenced by the host fragment. The MEP depicted in Fig. 8a has been computed from the ground state electron density of the nanotube alone. One can clearly see the polarization at both ends of the nanotube due to the passivation of the system with hydrogen atoms. The positive charge accumulated at the edges is balanced by an excess of negative charge distributed on the carbon atoms, mostly on the atoms directly bonded to

the hydrogens (this is also supported by the NPA, which attributes positive partial charges of 0.26 on each H atom and negative partial charges of  $-0.22$  on each connected C atom). The MEP shown in Fig. 8b has been obtained from the difference of the total system electron density and the  $\text{N}_3^-$  electron density computed in the basis of the total system, allowing us to appreciate the effect of the anion on the CNT charge distribution. In the central region of the nanotube, around the position of the anion, the charge of the nanotube flips sign and becomes positive. This is particularly evident from the bottom plot of Fig. 8b showing the value of the electrostatic potential inside the cavity. The sign flip does not occur everywhere, the carbon atoms at the edges remain negatively charged suggesting why during the geometry relaxation the  $\text{N}_3^-$  ion moved back to the midpoint of the nanotube. The positively charged hydrogens are shielded by the carbon atoms, making the CNT edge to effectively appear neutral to the  $\text{N}_3^-$  fragment, which tends to go to the midpoint of the nanotube where it can be most easily polarized.

We argue that the stabilization of the  $\text{N}_3^-$  moiety in the CNT cavity is largely due to electrostatic interactions. The confined ion induces a polarization on the nanotube, favored by the hydrogen passivation at both ends, causing a redistribution of the charge on the CNT wall such that the  $\text{N}_3^-$  fragment does not leave the cavity. Moreover, the diameter of the (5,5) CNT is such that the confined  $\text{N}_3^-$  azide anion lies at an optimal absorption distance from the wall surrounding it (in all directions), which makes it the most favorable host system among the nanotubes considered.

#### 4 Conclusions & Outlook

In this work we have studied the confinement of the azide anion inside finite-size single-wall zigzag and armchair CNTs of different diameters. It has been found that the N<sub>3</sub><sup>-</sup> anion is stabilized by nanotubes of diameters comprised between  $\approx 5.5$  Å and  $\approx 9.5$  Å, with the most favorable interaction energy of  $-32.31$  kcal/mol been obtained for a (5, 5) CNT with a diameter of  $\approx 6.78$  Å. The analysis of the relaxed structures, the natural atomic charges and the molecular electrostatic potential has revealed the possible nature of the interaction, suggesting an explanation of the results found. In particular, we argue that the guest N<sub>3</sub><sup>-</sup> molecule is stabilized by electrostatic interactions with the nanotube wall, undergoing a remarkable polarization catalyzed by the passivation of the nanotube edges through hydrogen atoms. The (5, 5) CNT allows the N<sub>3</sub><sup>-</sup> fragment to perfectly align itself in the center of the nanotube at an optimal distance from its wall in all directions, thus making it the best host system.

Although the N<sub>3</sub><sup>-</sup> azide anion is one of the most stable PNCs, the results obtained in this contribution are promising in the context of alternative energy storage and HEDM as an intermediate step toward the stabilization of more complex species which are energetically more appealing. In this moment, work is in progress in order to study the behavior of N<sub>5</sub> ionic species, N<sub>5</sub><sup>-</sup> and N<sub>5</sub><sup>+</sup> respectively, if they are placed in finite-size CNTs. The case of the cation is particularly interesting, since this almost linear molecule could be, in principle, hosted in CNTs similarly to the linear N<sub>3</sub><sup>-</sup>.

Preliminary results of this ionic species show a favorable unrelaxed interaction energy in the same order of magnitude as for the N<sub>3</sub><sup>-</sup> moiety, whereas the relaxation

process poses in this case some complications due to the high electron affinity of the cation. Indeed, it has been observed a considerable charge transfer from the nanotube wall to the nitrogen compound, altering significantly the  $N_5^+$  geometry, eventually leading to an undesired breaking of the molecule.

In order to avoid an excessive charge transfer from the CNT to the PNC, an anionic species could be inserted together with the  $N_5^+$  fragment. The existence of an ionic solid formed by  $N_3^-$  and  $N_5^+$  species has been subject to several theoretical studies, all predicting a low probability of success. Nonetheless, the recent theoretical findings of a stable polymeric  $N_8$  chain inside carbon and boron nitride nanotubes and stable  $N_n$  clusters inside a fullerene have suggested a new way to form stable polynitrogen compounds.

In particular, this approach could open the possibility to perform a reaction of the type  $N_3^- + N_5^+ \rightarrow N_8$  inside the nanotube, allowing the stabilization of more complex PNCs which does not directly dissociate to nitrogen molecules.

## 5 Acknowledgments

This work has been funded by the European Union's Horizon 2020 research and innovation programme under the Marie Skłodowska-Curie grant agreement n°642294. The calculations of this contribution have been performed under the grant 2016-p1048 at the HPC center CALMIP and the local computing cluster of the Laboratoire de Physique et Chimie Quantiques of Toulouse. N. F.-L. acknowledges financial support from Fondazione Cassa di Risparmio di Perugia (P 2014/1255, ACT 2014/6167). Finally, the authors wish to thank O. Brea for her contributions to the graphical material.

## References

1. Samartzis, P.C., Wodtke, A.M.: All-nitrogen chemistry: how far are we from N<sub>60</sub>? *Int. Rev. Phys. Chem.* **25**(4), 527–552 (2006). doi:10.1080/01442350600879319
2. Zarko, V.E.: Searching for Ways to Create Energetic Materials Based on Polynitrogen Compounds (Review). *Combust. Explos. Shock Waves* **46**(2), 121–131 (2010). doi:10.1007/s10573-010-0020-x
3. Curtius, T.: Ueber Stickstoffwasserstoffsäure (Azoimid) N<sub>3</sub>H. *Berichte der Dtsch. Chem. Gesellschaft* **23**(2), 3023–3033 (1890). doi:10.1002/cber.189002302232
4. Christe, K.O., Wilson, W.W., Sheehy, J.A., Boatz, J.A.: N<sub>5</sub><sup>+</sup>: A Novel Homoleptic Polynitrogen Ion as a High Energy Density Material. *Angew. Chemie Int. Ed.* **38**(13/14), 2004–2009 (1999). doi:10.1002/(SICI)1521-3773(19990712)38:13/14<2004::AID-ANIE2004>3.0.CO;2-7
5. Fau, S., Bartlett, R.J.: Possible Products of the End-On Addition of N<sub>3</sub><sup>-</sup> to N<sub>5</sub><sup>+</sup> and Their Stability. *J. Phys. Chem. A* **105**(16), 4096–4106 (2001). doi:10.1021/jp003970h
6. Gagliardi, L., Orlandi, G., Evangelisti, S., Roos, B.O.: A theoretical study of the nitrogen clusters formed from the ions N<sub>3</sub><sup>-</sup>, N<sub>5</sub><sup>+</sup>, and N<sub>5</sub><sup>-</sup>. *J. Chem. Phys.* **114**(24), 10,733–10,737 (2001). doi:10.1063/1.1370063
7. Evangelisti, S., Leininger, T.: Ionic nitrogen clusters. *J. Mol. Struct. THEOCHEM* **621**(1-2), 43–50 (2003). doi:10.1016/S0166-1280(02)00532-8
8. Dixon, D.A., Feller, D., Christe, K.O., Wilson, W.W., Vij, A., Vij, V., Jenkins, H.D.B., Olson, R.M., Gordon, M.S.: Enthalpies of Formation of Gas-Phase N<sub>3</sub>, N<sub>3</sub><sup>-</sup>, N<sub>5</sub><sup>+</sup>, and N<sub>5</sub><sup>-</sup> from Ab Initio Molecular Orbital Theory, Stability Predictions for N<sub>5</sub><sup>+</sup>N<sub>3</sub><sup>-</sup> and N<sub>5</sub><sup>+</sup>N<sub>5</sub><sup>-</sup>, and Experimental Evidence for the Instability of N<sub>5</sub><sup>+</sup>N<sub>3</sub><sup>-</sup>. *J. Am. Chem. Soc.* **126**(3), 834–843 (2004). doi:10.1021/ja0303182
9. Abou-Rachid, H., Hu, A., Timoshevskii, V., Song, Y., Lussier, L.S.: Nanoscale High Energetic Materials: A Polymeric Nitrogen Chain N<sub>8</sub> Confined inside a Carbon Nanotube. *Phys. Rev. Lett.* **100**(19), 196,401 (2008). doi:10.1103/PhysRevLett.100.196401
10. Ji, W., Timoshevskii, V., Guo, H., Abou-Rachid, H., Lussier, L.: Thermal stability and formation barrier of a high-energetic material N<sub>8</sub> polymer nitrogen encapsulated in (5,5) carbon nanotube. *Appl. Phys. Lett.* **95**(2), 021,904 (2009). doi:10.1063/1.3162334

11. Zheng, F., Yang, Y., Zhang, P.: Polymeric Nitrogen Chains Confined in Carbon Nanotube Bundle. *Int. J. Mod. Phys. B* **26**(18), 1250,047 (2012). doi:10.1142/S0217979212500476
12. Liu, S., Yao, M., Ma, F., Liu, B., Yao, Z., Liu, R., Cui, T., Liu, B.: High Energetic Polymeric Nitrogen Stabilized in the Confinement of Boron Nitride Nanotube at Ambient Conditions. *J. Phys. Chem. C* **120**(30), 16,412–16,417 (2016). doi:10.1021/acs.jpcc.6b04374
13. Wu, Z., Benchafia, E.M., Iqbal, Z., Wang, X.:  $N_8^-$  Polynitrogen Stabilized on Multi-Wall Carbon Nanotubes for Oxygen-Reduction Reactions at Ambient Conditions. *Angew. Chemie - Int. Ed.* **126**, 12,763–12,767 (2014). doi:10.1002/anie.201403060
14. Sharma, H., Garg, I., Dharamvir, K., Jindal, V.K.: Structure of Polynitrogen Clusters Encapsulated in  $C_{60}$ : A Density Functional Study. *J. Phys. Chem. C* **114**(19), 9153–9160 (2010). doi:10.1021/jp908755r
15. Xu, B., Pan, B.C.: Study of Gallium Fragments Encapsulated in Single-Walled Carbon Nanotubes. *J. Phys. Chem. C* **113**(2), 567–570 (2009). doi:10.1021/jp807477a
16. Garg, I., Sharma, H., Dharamvir, K., Jindal, V.K.: DFT Study of  $Al_n$  (1-13) Clusters Encapsulated Inside Single Walled Carbon Nanotubes. *J. Phys. Chem. C* **114**(44), 18,762–18,772 (2010). doi:10.1021/jp1036475
17. Becke, A.D.: Density-functional exchange-energy approximation with correct asymptotic behavior. *Phys. Rev. A* **38**(6), 3098–3100 (1988). doi:10.1103/PhysRevA.38.3098
18. Becke, A.D.: Density-functional thermochemistry. III. The role of exact exchange. *J. Chem. Phys.* **98**(7), 5648–5652 (1993). doi:10.1063/1.464913
19. Lee, C., Yang, W., Parr, R.G.: Development of the Colle-Salvetti correlation-energy formula into a functional of the electron density. *Phys. Rev. B* **37**(2), 785–789 (1988). doi:10.1103/PhysRevB.37.785
20. Hehre, W.J., Ditchfield, R., Stewart, R.F., Pople, J.A.: Self-Consistent Molecular-Orbital Methods. I. Use of Gaussian Expansions of Slater-Type Atomic Orbitals. *J. Chem. Phys.* **51**(6), 2657–2664 (1969). doi:10.1063/1.1673374
21. Boys, S.F., Bernardi, F.: The calculation of small molecular interactions by the differences of separate total energies. Some procedures with reduced errors. *Mol. Phys.* **19**(4), 553–566 (1970). doi:10.1080/00268977000101561
22. Austin, A., Petersson, G.A., Frisch, M.J., Dobek, F.J., Scalmani, G., Throssell, K.: A Density Functional with Spherical Atom Dispersion Terms. *J. Chem. Theory Comput.*

- 8(12), 4989–5007 (2012). doi:10.1021/ct300778e
23. Werner, H.J., Knowles, P.J., Knizia, G., Manby, F.R., Schütz, M.: Molpro: A general-purpose quantum chemistry program package. *Wiley Interdiscip. Rev. Comput. Mol. Sci.* **2**(2), 242–253 (2012). doi:10.1002/wcms.82
24. Werner, H.J., Knowles, P.J., Knizia, G., Manby, F.R., Schütz, M., Celani, P., Györfy, W., Kats, D., Korona, T., Lindh, R., Mitrushenkov, A.O., Rauhut, G., Shamasundar, K.R., Adler, T.B., Amos, R.D., Bernhardsson, A., Berning, A., Cooper, D.L., Deegan, M.J.O., Dobbyn, A.J., Eckert, F., Goll, E., Hampel, C., Hesselmann, A., Hetzer, G., Hrenar, T., Jansen, G., Köppl, C., Liu, Y., Lloyd, A.W., Mata, R.A., May, A.J., McNicholas, S.J., Meyer, W., Mura, M.E., Nicklass, A., O’Neill, D.P., Palmieri, P., Peng, D., Pflüger, K., Pitzer, R., Reiher, M., Shiozaki, T., Stoll, H., Stone, A.J., Tarroni, R., Thorsteinsson, T., Wang, M.: MOLPRO, version 2015.1, a package of ab initio programs (2015). URL <http://www.molpro.net>
25. Frisch, M.J., Trucks, G.W., Schlegel, H.B., Scuseria, G.E., Robb, M.A., Cheeseman, J.R., Scalmani, G., Barone, V., Mennucci, B., Petersson, G.A., Nakatsuji, H., Caricato, M., Li, X., Hratchian, H.P., Izmaylov, A.F., Bloino, J., Zheng, G., Sonnenberg, J.L., Hada, M., Ehara, M., Toyota, K., Fukuda, R., Hasegawa, J., Ishida, M., Nakajima, T., Honda, Y., Kitao, O., Nakai, H., Vreven, T., Montgomery Jr., J.A., Peralta, J.E., Ogliaro, F., Bearpark, M., Heyd, J.J., Brothers, E., Kudin, K.N., Staroverov, V.N., Kobayashi, R., Normand, J., Raghavachari, K., Rendell, A., Burant, J.C., Iyengar, S.S., Tomasi, J., Cossi, M., Rega, N., Millam, J.M., Klene, M., Knox, J.E., Cross, J.B., Bakken, V., Adamo, C., Jaramillo, J., Gomperts, R., Stratmann, R.E., Yazyev, O., Austin, A.J., Cammi, R., Pomelli, C., Ochterski, J.W., Martin, R.L., Morokuma, K., Zakrzewski, V.G., Voth, G.A., Salvador, P., Dannenberg, J.J., Dapprich, S., Daniels, A.D., Farkas, Ö., Foresman, J.B., Ortiz, J.V., Cioslowski, J., Fox, D.J.: Gaussian 09 Revision D.01. URL <http://www.gaussian.com>
26. Glendening, E.D., Badenhoop, J.K., Reed, A.D., Carpenter, J.E., Weinhold, F.: NBO Version 3.1
27. Avogadro: an open-source molecular builder and visualization tool. Version 1.2.0. URL <http://avogadro.cc/>

- 
28. Hanwell, M.D., Curtis, D.E., Lonie, D.C., Vandermeersch, T., Zurek, E., Hutchison, G.R.: Avogadro: an advanced semantic chemical editor, visualization, and analysis platform. *J. Cheminform.* **4**(1), 17 (2012). doi:10.1186/1758-2946-4-17
  29. Dennington, R., Keith, T., Millam, J.: *GaussView Version 5* (2009)
  30. Reed, A.E., Weinstock, R.B., Weinhold, F.: Natural population analysis. *J. Chem. Phys.* **83**(2), 735–746 (1985). doi:10.1063/1.449486

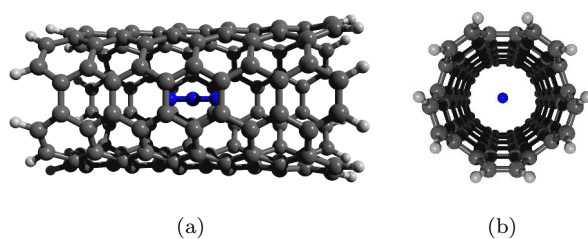


**Fig. 1** Example geometry of N<sub>3</sub><sup>-</sup> confined inside a (5,5) CNT used to compute unrelaxed interaction energies

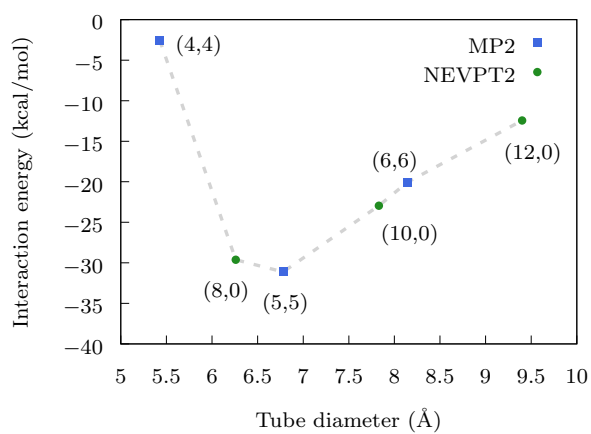


**Fig. 2** Unrelaxed interaction energies

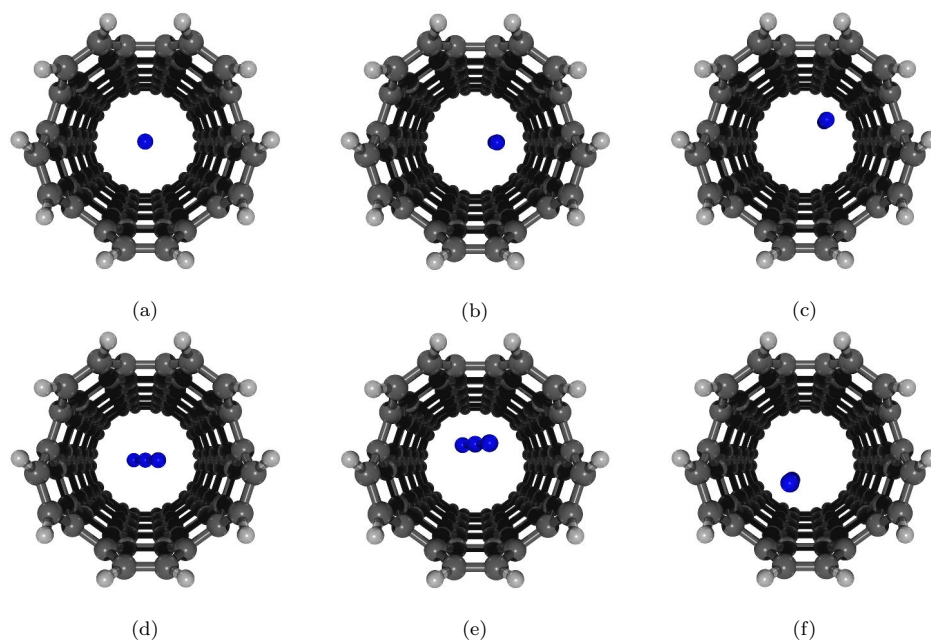


**Fig. 3** Starting orientations of  $N_3^-$  inside a (5,5) CNT prior the geometry relaxation. In the last two cases (e) and (f), the  $N_3^-$  ion is closer to the edge of the CNT, while in all other cases is placed in the midpoint

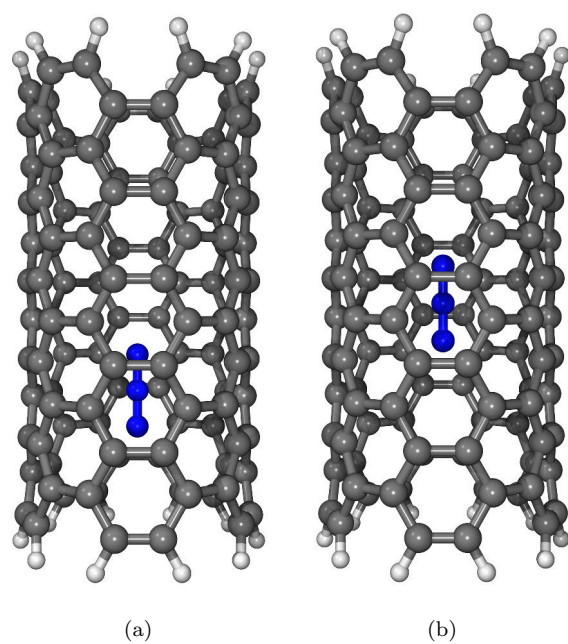


**Fig. 4** Starting (a) and final (b) position of the  $N_3^-$  ion inside the CNT

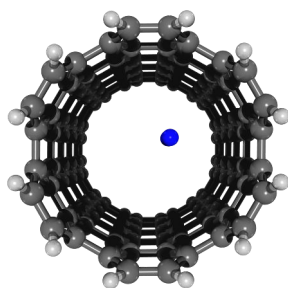


**Fig. 5** Relaxed geometry of  $N_3^-$  confined inside a (6,6) CNT

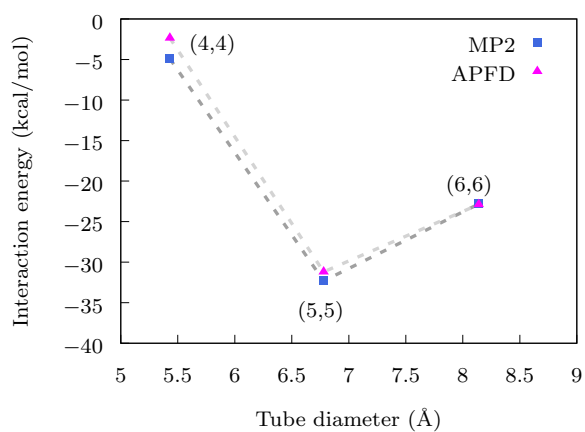


**Fig. 6** Relaxed interaction energies

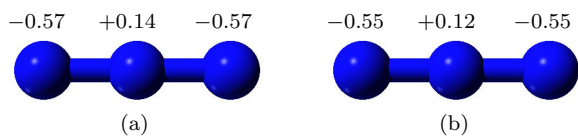


**Fig. 7** Partial atomic charges for the  $N_3^-$  fragment outside (a) and inside a (5,5) CNT (b)

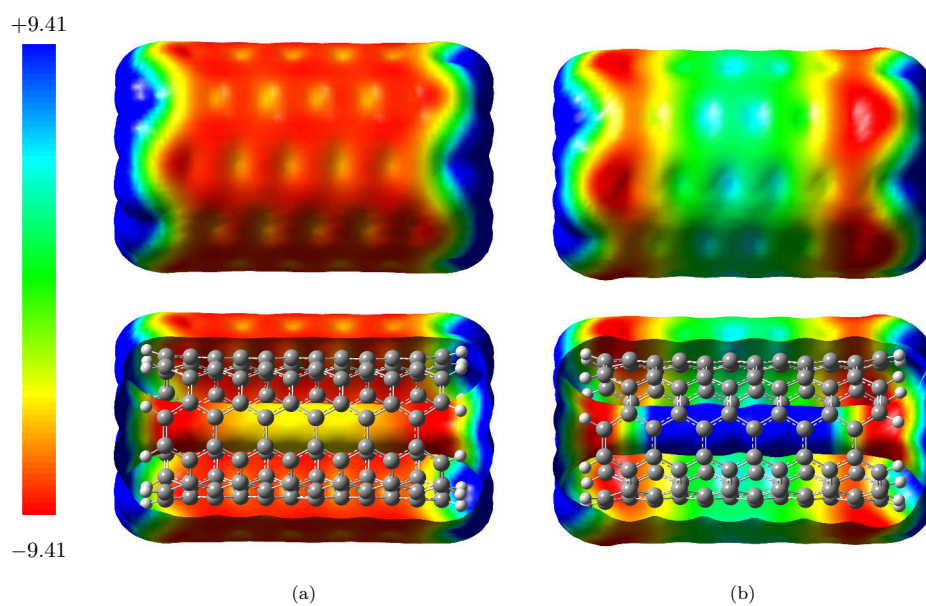


**Fig. 8** Electrostatic potential map of the (5,5) CNT unperturbed (a) and perturbed by the presence of the N<sub>3</sub><sup>-</sup> molecule (b). Isosurface value of the electron density set to 0.02 and energy scale given in kcal/mol